JRAEE

Journal of Robotics, Automation, and Electronics Engineering
Vol. 3, No. 2, 2025, pp. 165-177
e-ISSN 3025-3780
https://journal.uny.ac.id/v3/jraee

# Attitude Stabilization of a Tricopter UAV Using Integral-Augmented Linear Quadratic Regulation

Dika Saputra[a,1], Oktaf Agni Dhewa[b,2,*]

[a,b]Dept. of Electrical and Electronic Engineering, Vocational Faculty, Universitas Negeri Yogyakarta
[1]dikasaputra.2020@student.uny.ac.id; [2]oktafagnidhewa@uny.ac.id
[*] Corresponding Author

**ARTICLE INFO**

**Article History**
Received Date Month Year
Revised Date Month Year
Accepted Date Month Year

## ABSTRACT

Attitude stabilization of a tricopter unmanned aerial vehicle (UAV) is challenging because its asymmetric three-rotor configuration and servo-actuated rear rotor introduce coupled and disturbance-sensitive rotational dynamics. This study develops and experimentally evaluates an integral-augmented Linear Quadratic Regulator (LQR-I) for roll, pitch, and yaw stabilization of a physical tricopter UAV. The controller was implemented on an embedded flight controller using inertial measurements from an MPU6050 and was evaluated through tuning-rig experiments and outdoor free-flight tests under measured wind disturbances. A conventional LQR was used as the baseline controller. To ensure a consistent comparison, the performance of both controllers was evaluated under the same measured wind speed of 4.4 m/s. Under this condition, LQR-I reduced pitch overshoot from 9.03° to 2.85° and yaw overshoot from 13.43° to 3.35°, corresponding to reductions of approximately 68.4% and 75.1%, respectively. Roll overshoot increased slightly from 5.25° to 5.47°. The magnitude of the steady-state error was reduced by approximately 56.6%, 16.6%, and 50.6% for the roll, pitch, and yaw axes, respectively. In addition, the root mean square error (RMSE) decreased from 2.451° to 2.065° for roll, from 3.397° to 2.542° for pitch, and from 2.744° to 1.227° for yaw. These experimental results demonstrate that integral augmentation improves the overall disturbance-rejection and attitude-tracking performance of the tricopter, particularly in the pitch and yaw axes, although a slight increase in roll overshoot was observed.

**Keywords**
Tricopter;
Unmanned Aerial Vehicle;
Linear Quadratic Regulator;
Integral Augmentation;
Attitude Stabilization.

## ABSTRAK

Stabilisasi sikap terbang (*attitude*) pada *unmanned aerial vehicle* (UAV) jenis tricopter merupakan tantangan karena konfigurasi tiga rotor yang tidak simetris dan mekanisme servo pada rotor belakang menghasilkan dinamika rotasi yang saling terkopel serta sensitif terhadap gangguan. Penelitian ini mengembangkan dan mengevaluasi secara eksperimental *Linear Quadratic Regulator* dengan penambahan aksi integral (LQR-I) untuk menstabilkan gerak roll, pitch, dan yaw pada tricopter fisik. Kendali diimplementasikan pada *flight controller* tertanam menggunakan pengukuran inersial dari MPU6050 dan dievaluasi melalui pengujian *tuning rig* serta pengujian terbang bebas di luar ruangan dengan gangguan angin yang diukur. LQR konvensional digunakan sebagai kendali pembanding. Untuk memperoleh

ISSN 3025-3780 (online)
ISSN 3025-4590 (printed)

perbandingan yang konsisten, performa kedua kendali dibandingkan pada kecepatan angin yang sama, yaitu 4,4 m/s. Pada kondisi tersebut, LQR-I menurunkan overshoot pitch dari 9,03° menjadi 2,85° dan overshoot yaw dari 13,43° menjadi 3,35°, atau masing-masing sekitar 68,4% dan 75,1%. Overshoot roll mengalami sedikit peningkatan dari 5,25° menjadi 5,47°. Magnitudo *steady-state error* menurun sekitar 56,6%, 16,6%, dan 50,6% pada sumbu roll, pitch, dan yaw. Nilai *root mean square error* (RMSE) juga menurun dari 2,451° menjadi 2,065° pada roll, dari 3,397° menjadi 2,542° pada pitch, serta dari 2,744° menjadi 1,227° pada yaw. Hasil eksperimen menunjukkan bahwa penambahan aksi integral pada LQR meningkatkan kemampuan penolakan gangguan dan akurasi kendali sikap tricopter secara keseluruhan, khususnya pada sumbu pitch dan yaw, meskipun terdapat sedikit peningkatan overshoot pada sumbu roll.



## 1. Introduction

Unmanned aerial vehicles (UAVs) have become important aerial platforms for autonomous and remotely operated missions because of their flexibility, relatively low operating cost, and ability to operate in environments that may be difficult or hazardous for conventional systems. As UAV autonomy increases, reliable flight-control systems capable of maintaining stable attitude and position under nonlinear dynamics, modeling uncertainties, actuator limitations, and environmental disturbances become increasingly important. Recent surveys of multirotor UAV control have investigated a broad range of approaches, including proportional–integral–derivative (PID), Linear Quadratic Regulator (LQR), sliding-mode control, Model Predictive Control (MPC), adaptive control, and hybrid control methods [1].

Among multirotor configurations, tricopters employ three main propulsion units and typically use a Y-shaped airframe. In a conventional single-tilt configuration, the rear propulsion unit is mechanically tilted by a servo actuator to generate yaw-control torque. Although this configuration uses fewer main propulsion units than a quadrotor, the asymmetric arrangement and rear-rotor vectoring mechanism introduce additional coupling among thrust generation, yaw actuation, and vehicle attitude dynamics. Recent tricopter studies have therefore emphasized the importance of accurate dynamic modeling, control allocation, and disturbance compensation for maintaining stable attitude and hovering performance [2], [3].

Attitude stabilization is particularly important because deviations in roll, pitch, and yaw alter the orientation of the total thrust vector and consequently influence the translational motion of the UAV. External disturbances such as wind, actuator asymmetry, payload variation, mechanical backlash, and modeling uncertainty may produce persistent angular deviations and oscillatory responses. These effects are particularly relevant to tricopters because yaw regulation strongly depends on the mechanical and dynamic behavior of the servo-actuated rear rotor.

LQR provides a systematic state-feedback framework in which the feedback gains are determined by minimizing a quadratic performance index that balances state deviation and control effort. Previous studies have demonstrated that LQR can provide fast and well-damped multirotor attitude responses while maintaining relatively low computational complexity [4], [5]. Nevertheless, conventional state-feedback LQR does not inherently guarantee zero steady-state tracking error in the presence of constant disturbances, actuator mismatch, parameter uncertainty, or unmodeled dynamics.

Integral augmentation provides a practical mechanism for reducing persistent tracking error by accumulating the difference between the desired and measured states and introducing an additional corrective action. Experimental investigations have demonstrated that optimal state feedback combined with integral action can improve steady-state accuracy and disturbance rejection in multirotor systems. Godínez-Garrido et al. experimentally demonstrated an integral optimal controller for quadrotor attitude and altitude stabilization under deliberately introduced crosswind disturbances [6]. Ahmad and Fareed evaluated an integral-based LQR controller on a real-time three-degree-of-freedom UAV test bench and reported improved transient performance compared with basic LQR control [7]. Integral compensation has also been applied to autonomous waypoint tracking, where it reduced steady-state error and repeated overshoot compared with conventional LQR [8].

Recent developments have extended conventional LQR using adaptive and learning-based methods to compensate for changes in UAV dynamics and operating conditions. Online adjustment of LQR gains using neural-network-based approaches, for example, has demonstrated improvements in attitude regulation under varying environmental conditions [9]. Adaptive weighting-matrix selection has also been investigated to improve the tracking and robustness characteristics of LQR-based UAV control [10].

However, most experimental investigations of integral-augmented LQR have focused on quadrotor platforms. Experimental evaluation on a conventional single-tilt tricopter remains comparatively limited. The asymmetric propulsion arrangement and servo-actuated yaw mechanism of a tricopter create rotational characteristics that differ from those of symmetric quadrotors. Consequently, the effectiveness of integral augmentation should be experimentally evaluated on the tricopter platform rather than inferred directly from quadrotor results.

Accordingly, this study implements and experimentally evaluates an integral-augmented Linear Quadratic Regulator (LQR-I) for attitude stabilization of a physical tricopter UAV. The proposed controller regulates the roll, pitch, and yaw motions using inertial measurements from an onboard MPU6050 sensor. Controller performance is first evaluated using an attitude tuning rig and subsequently validated through outdoor free-flight experiments under measured natural wind disturbances. A conventional LQR is used as the baseline controller. Overshoot, steady-state error, and root mean square error (RMSE) are used as the primary performance metrics, with the principal controller comparison conducted under an identical measured wind speed of 4.4 m/s.

## 2. Research Method

### 2.1 Tricopter Hardware Design

The experimental UAV employs a Y-shaped tricopter configuration, as illustrated in Fig. 1. Three hollow carbon-fiber arms with a length of approximately 20 cm form the primary structure of the vehicle. Carbon fiber was selected because it provides a lightweight structure with sufficient mechanical stiffness for supporting the propulsion units.

Each propulsion unit consists of a 980 KV brushless DC motor, an HQProp 10 × 4.5 inch propeller, and an electronic speed controller (ESC). The two front propulsion units are mounted in fixed orientations, whereas the rear propulsion unit is mounted on a servo-actuated tilt mechanism. The rear servo changes the thrust-vector direction to generate the torque required for yaw regulation.

The central body accommodates the battery, flight controller, radio receiver, telemetry module, power-regulation components, and inertial sensor. Structural components of the main body were manufactured using three-dimensional printing to provide compact accommodation for the electronics and propulsion wiring.

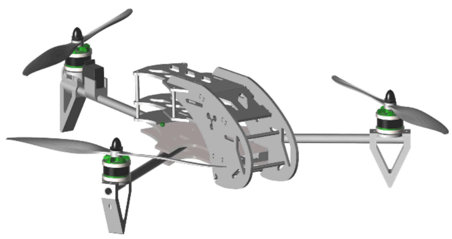

**Fig. 1** Mechanical design of the tricopter UAV

### 2.2 Electronic Architecture

The electronic architecture of the tricopter is shown in Fig. 2. A Teensy-based embedded microcontroller serves as the central flight-control unit and executes the attitude-control algorithm in real time. The MPU6050 inertial measurement unit provides three-axis accelerometer and gyroscope measurements and communicates with the flight controller through an I²C interface.

Pilot commands are transmitted from the radio controller to an onboard receiver and subsequently acquired by the flight controller. Based on the reference commands and measured attitude states, the controller calculates the required corrections for the three propulsion units and the rear tilt servo.

ISSN 3025-3780 (online)
ISSN 3025-4590 (printed)

The three ESCs receive pulse-width modulation (PWM) commands from the flight controller and regulate the rotational speeds of the brushless motors. An additional PWM output controls the rear servo for yaw actuation. A 433 MHz telemetry module connected through a serial interface transfers sensor measurements and controller data to a ground station for real-time monitoring and experimental data recording.

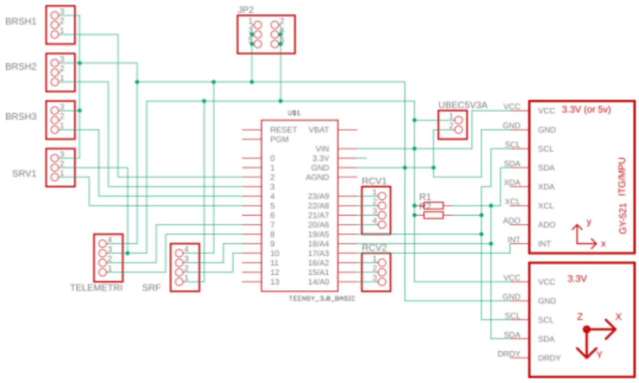


**Fig. 2** Electronic architecture of the tricopter UAV

## 2.3 Flight-Control Software

The flight-control software was developed in C++ using the Arduino development environment. The overall program flow is illustrated in Fig. 3. During initialization, the program declares the required variables and configures the inertial sensor, receiver, ESC outputs, rear servo, and telemetry interface.

During flight, accelerometer and gyroscope measurements are continuously acquired from the MPU6050. The sensor measurements are processed to obtain the roll, pitch, and yaw states and their corresponding angular rates. Pilot reference commands are subsequently compared with the measured attitude st

Depending on the experimental configuration, the resulting state information is supplied either to the conventional LQR or the integral-augmented LQR controller. The calculated control outputs are converted into PWM commands for the three ESCs and rear tilt servo. Relevant flight variables are simultaneously transmitted through the telemetry link for subsequent analysis.

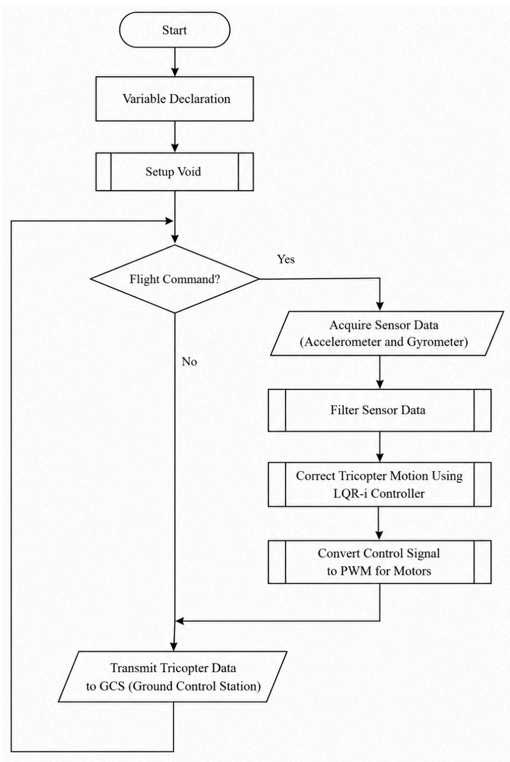


**Fig. 3** Flight-control program flowchart

### 2.4 Linearized Attitude Model and Conventional LQR

Around the hovering operating condition and for relatively small angular deviations, each rotational axis can be represented using a linearized second-order model. For an attitude variable $\eta_i$, representing roll φ, pitch θ, or yaw ψ, the state vector is defined as,

$$x_i = [\eta_i \quad \dot{\eta}_i]^T \tag{1}$$

The linearized dynamics are represented by

$$\dot{x}_i = A_i x_i + B_i u_i \tag{2}$$

and the system output is expressed as

$$y_i = C_i x_i \tag{3}$$

where $u_i$ represents the control input associated with the corresponding rotational axis. The conventional LQR feedback gain is determined by minimizing the quadratic performance index

$$J = \int_0^\infty \left( x_i^T Q_i x_i + u_i^T R_i u_i \right) dt \tag{4}$$

where $Q_i$ represents the state-weighting matrix and $R_i$ determines the penalty associated with control effort. The resulting state-feedback control law is

$$u_i = -K_i x_i \tag{5}$$

where $K_i$ is obtained by solving the corresponding Algebraic Riccati Equation (ARE). The conventional LQR controller was subsequently used as the baseline controller during outdoor free-flight experiments.

### 2.5 Integral-Augmented LQR Design

Conventional LQR state feedback may produce residual tracking errors when persistent disturbances or unmodeled effects are present. To reduce this error, an integral state was introduced into each attitude-control channel. For each rotational axis, the integral error is defined as

$$\xi_i(t) = \int_0^t [r_i(\tau) - y_i(\tau)]\, d\tau \tag{6}$$

where $r_i$ represents the reference attitude and $y_i$ is the measured attitude response. The augmented state vector is then expressed as

$$x_{a,i} = [x_i^T \quad \xi_i]^T \tag{7}$$

and the augmented system becomes

$$\begin{bmatrix} \dot{x}_i \\ \dot{\xi}_i \end{bmatrix} = \begin{bmatrix} A_i & 0 \\ -C_i & 0 \end{bmatrix} \begin{bmatrix} x_i \\ \xi_i \end{bmatrix} + \begin{bmatrix} B_i \\ 0 \end{bmatrix} u_i + \begin{bmatrix} 0 \\ I \end{bmatrix} r_i \tag{8}$$

where the corresponding augmented matrices can be represented as

$$A_{a,i} = [A_i \quad 0 - C_i \quad 0] \tag{9}$$

and

$$E_{a,i} = \begin{bmatrix} 0 \\ I \end{bmatrix} \tag{10}$$

The integral-augmented controller minimizes the augmented quadratic performance index

$$J_a = \int_0^\infty \left( x_{a,i}^T Q_{a,i} x_{a,i} + u_i^T R_i u_i \right) dt \tag{11}$$

The corresponding control law can be expressed as

$$u_i = -K_{x,i} x_i - K_{i,I} \xi_i \tag{12}$$

where $K_{x,i}$ is the state-feedback gain and $K_i$,I is the integral compensation gain. For the roll-axis design, the weighting parameters were selected as

$$Q_\phi = \text{diag}\left([500 \quad 0.05]\right), \qquad R_\phi = 1 \tag{13}$$

The MATLAB-based augmented-controller analysis produced a state-feedback component of

$$K_{x,\phi} = [22.3988 \quad 0.8533] \tag{14}$$

Journal of Robotics, Automation, and Electronics Engineering
Vol. 3, No. 2, 2025, pp. 165-177
ISSN 3025-3780 (online)
ISSN 3025-4590 (printed)

and an initial integral component that was subsequently refined experimentally. Based on tuning-rig evaluation, the practical roll integral gain was selected as

$$K_{\phi,I} = 0.0140 \tag{15}$$

The weighting parameters used for the pitch axis were

$$Q_\theta = \mathrm{diag}(400, 0.25), R_\theta = 1 \tag{16}$$

while the yaw-axis parameters were

$$Q_\psi = \mathrm{diag}(250, 0.20), R_\psi = 1 \tag{17}$$

The pitch and yaw integral gains were subsequently adjusted experimentally using the same tuning-rig procedure. Their final standalone values were not separately documented in the original experimental records; therefore, numerical values are not assigned to these gains in this manuscript.

The resulting LQR-I controller combines state feedback with accumulated attitude error, thereby providing additional corrective action against persistent disturbances and actuator-related biases. The complete control architecture is illustrated in Fig. 4.

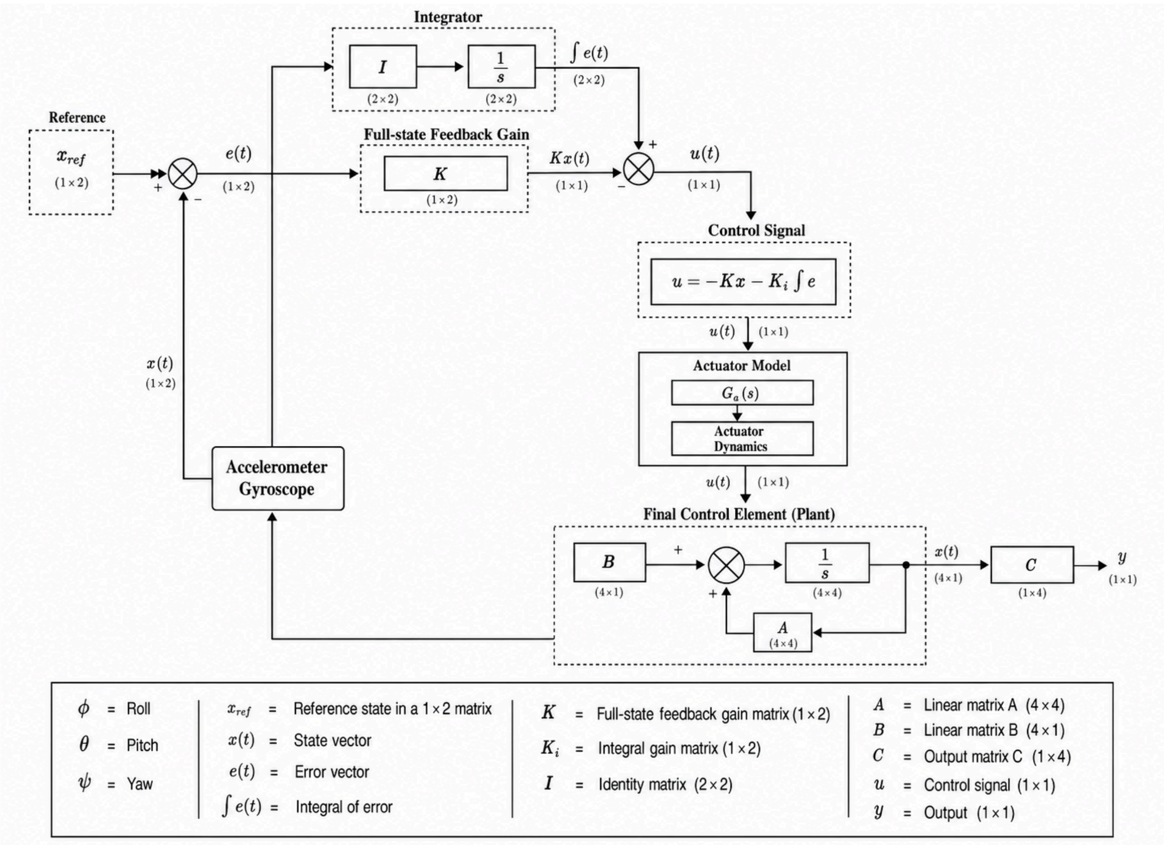


**Fig. 4** Integral-augmented LQR attitude-control architecture

## 2.6 Experimental Procedure

The experimental evaluation consisted of three stages. First, the LQR-I controller was evaluated on an attitude tuning rig. Five repeated trials were conducted for each rotational axis to characterize rise time, settling time, overshoot, and steady-state error.

Second, outdoor free-flight tests were conducted using the conventional LQR controller. Natural wind was used as the external disturbance, and wind velocity was measured using an anemometer. The conventional LQR was evaluated under wind speeds of approximately 3.4 m/s and 4.4 m/s.

Third, the LQR-I controller was evaluated through outdoor free-flight experiments under measured wind speeds of approximately 2.6 m/s and 4.4 m/s. Because the lower-wind experiments were conducted at different disturbance levels for LQR and LQR-I, they were not used for direct quantitative comparison. The main controller comparison was therefore based exclusively on experiments conducted at the common wind speed of 4.4 m/s.

The roll, pitch, and yaw attitude references were approximately 0° during the stability experiments. Performance was evaluated using overshoot, steady-state error, and root mean square error. RMSE is calculated as

$$\text{RMSE} = \sqrt{\frac{1}{N}\sum_{k=1}^{N} e_k^2} \tag{18}$$

where e□ represents the attitude tracking error at sample k and N is the total number of samples.

## 3. Result and Discussion

### 3.1 Hardware and Software Implementation

The mechanical and electronic components were integrated into the physical tricopter as shown in Figs. 5 and 6. The flight controller, battery, receiver, power-regulation module, telemetry system, ESCs, and inertial sensor were located within the central structure, while the three 980 KV brushless motors were mounted on the corresponding arms.

The rear propulsion unit was mechanically coupled to a servo-actuated tilt mechanism used for yaw control. The implemented flight-control software executed sensor acquisition, attitude estimation, LQR/LQR-I computation, actuator command generation, and telemetry transmission in real time.

The controller gain matrices and corresponding parameters were stored in the embedded software, while the resulting controller outputs were combined with the pilot commands and subsequently converted to PWM signals for the propulsion motors and rear servo.

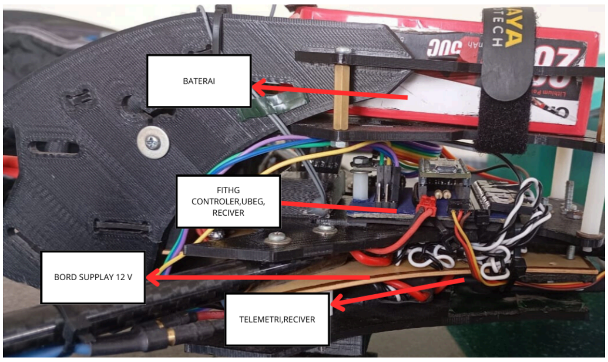


**Fig. 5** Placement of electronic components

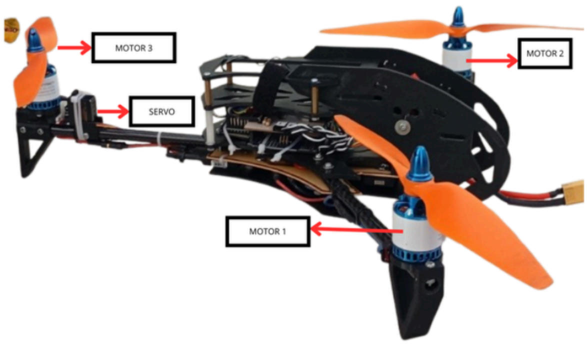


**Fig. 6** Placement of brushless motors and rear tilt servo

### 3.2 LQR-I Evaluation Using the Tuning Rig

#### 3.2.1 Roll-Axis Response

Five repeated roll-axis experiments were conducted using the tuning rig.

Journal of Robotics, Automation, and Electronics Engineering
Vol. 3, No. 2, 2025, pp. 165-177
ISSN 3025-3780 (online)
ISSN 3025-4590 (printed)

**Table 1**. Roll-axis Response Characteristics Using LQR-I

| Parameter | Test 1 | Test 2 | Test 3 | Test 4 | Test 5 | Minimum Requirement |
|---|---|---|---|---|---|---|
| Rise time (s) | 0.4 | 0.2 | 0.3 | 0.5 | 0.6 | < 1s |
| Settling time (s) | 0.9 | 1.0 | 1.1 | 1.2 | 0.9 | < 3s |
| Overshoot (°) | 8.88 | 9.18 | 4.23 | 26.47 | 25.79 | ±9% |
| Steady-State Error (°) | 1.74 | 1.46 | -0.59 | -0.12 | -1.89 | < ±4.5° |

Across the five experiments, the roll controller achieved a mean rise time of approximately 0.40 ± 0.16 s and a mean settling time of 1.02 ± 0.13 s. However, the mean overshoot was 14.91 ± 10.43°, indicating substantial trial-to-trial variability.

Tests 4 and 5 produced overshoots considerably above the predefined requirement, whereas the steady-state error remained within ±4.5° in all five experiments. These results indicate that integral augmentation provided acceptable steady-state roll regulation, although the transient response remained sensitive to experimental conditions during tuning.

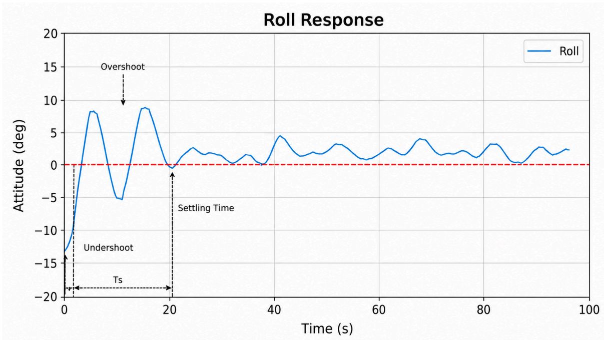


**Fig. 7** Roll response during tuning-rig testing

### 3.2.2 Pitch-Axis Response

The pitch-axis test results are summarized in Table 2.

**Table 2**. Pitch-axis Response Characteristics Using LQR-I

| Parameter | Test 1 | Test 2 | Test 3 | Test 4 | Test 5 | Minimum Requirement |
|---|---|---|---|---|---|---|
| Rise time (s) | 1.4 | 1.7 | 0.1 | 1.2 | 0.9 | < 1s |
| Settling time (s) | 0.9 | 0.9 | 0.5 | 0.9 | 0.5 | < 3s |
| Overshoot (°) | 2.92 | 2.72 | 28.32 | 4.68 | 19.00 | ±9% |
| Steady-State Error (°) | 1.26 | -0.06 | -1.40 | -1.41 | -1.11 | < ±4.5° |

The mean rise time was approximately 1.06 ± 0.61 s, while the mean settling time was 0.74 ± 0.22 s. Considerable variation was observed in overshoot, particularly in Tests 3 and 5.

Despite the transient variability, the steady-state error remained within the ±4.5° requirement for all tests. Therefore, as observed for the roll axis, the principal limitation during pitch tuning was transient repeatability rather than steady-state accuracy.

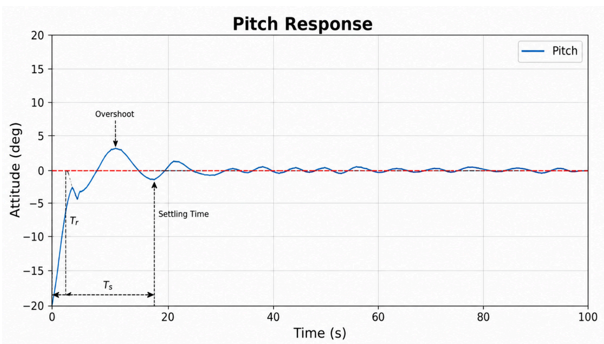


**Fig. 8** Pitch response during tuning-rig testing

### 3.2.3 Yaw-Axis Response

The yaw-axis response showed greater repeatability than the roll and pitch responses.

**Table 3**. Yaw-axis Response Characteristics Using LQR-I

| Parameter | Test 1 | Test 2 | Test 3 | Test 4 | Test 5 | Minimum Requirement |
|---|---|---|---|---|---|---|
| Rise time (s) | 0.6 | 0.6 | 0.5 | 0.7 | 0.5 | < 1s |
| Settling time (s) | 0.5 | 0.6 | 0.5 | 0.7 | 0.6 | < 3s |
| Overshoot (°) | 3.00 | 5.16 | 7.15 | 3.26 | 5.92 | ±9% |
| Steady-State Error (°) | -2.28 | -0.33 | -0.24 | -0.83 | -0.22 | < ±4.5° |

The mean rise time and settling time were both approximately 0.58 ± 0.08 s, while the mean overshoot was approximately 4.90 ± 1.77°. All five yaw tests satisfied the predefined rise-time, settling-time, overshoot, and steady-state-error requirements. These results indicate that the LQR-I configuration produced relatively consistent yaw stabilization on the tuning rig.

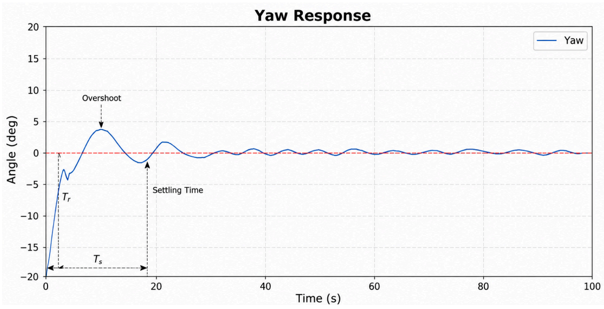


**Fig. 9** Yaw response during tuning-rig testing

## 3.3 Outdoor Flight Tests Using Conventional LQR

Outdoor free-flight experiments were initially conducted using the conventional LQR controller to establish baseline attitude performance under naturally occurring wind disturbances.

At a measured wind speed of approximately 3.4 m/s, the tricopter maintained bounded roll, pitch, and yaw motion around the corresponding reference attitudes. The experimental responses are shown in Fig. 10.

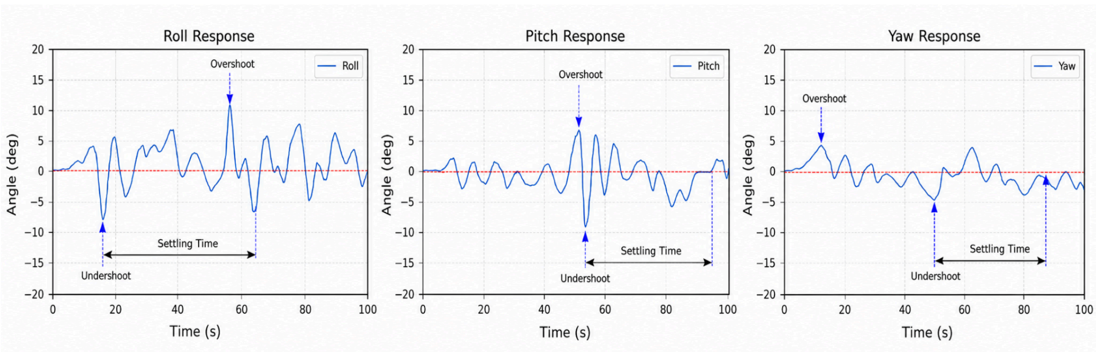


**Fig. 10** Roll, pitch, and yaw response using LQR under a wind speed of 3.4 m/s

A second conventional-LQR flight experiment was conducted under a measured wind speed of 4.4 m/s. Under this condition, the recorded overshoot values were 5.25°, 9.03°, and 13.43° for roll, pitch, and yaw, respectively.

The corresponding steady-state errors were 1.909°, 2.429°, and 1.796°, while the RMSE values were 2.451°, 3.397°, and 2.744°. The yaw axis exhibited the largest overshoot, indicating that the rear-rotor yaw-control mechanism was particularly sensitive to the higher wind disturbance. Although the conventional LQR maintained bounded attitude motion, the relatively large yaw transient and residual errors provided a clear baseline for evaluating the effect of integral augmentation.

ISSN 3025-3780 (online)
ISSN 3025-4590 (printed)

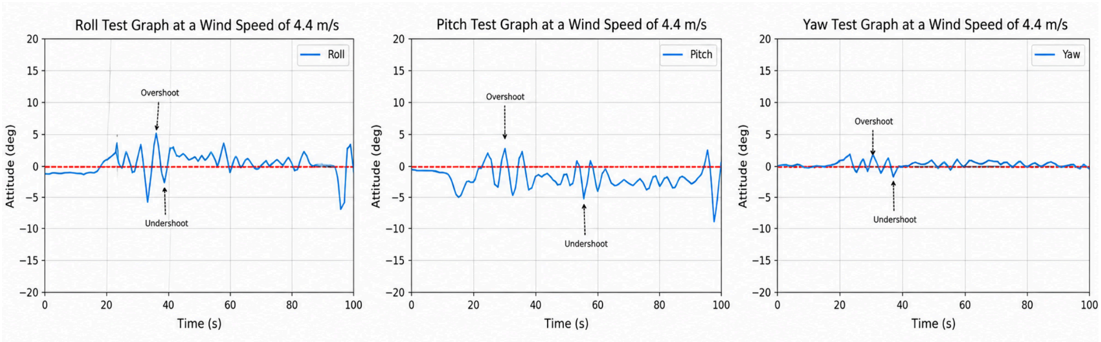


**Fig. 11** Roll, pitch, and yaw response using LQR under a wind speed of 4.4 m/s

## 3.4 Outdoor Flight Tests Using LQR-I

### 3.4.1 Flight Test at 2.6 m/s Wind Speed

The LQR-I controller was first evaluated under a measured wind speed of approximately 2.6 m/s.

**Table 4**. LQR-I Flight Performance Under a Wind Speed of 2.6 m/s

| Parameter | Roll | Pitch | Yaw |
|---|---|---|---|
| Overshoot (°) | 4.14 | 1.68 | 2.43 |
| Steady-State Error (°) | 0.69 | -1.86 | 0.48 |
| RMSE (°) | 1.54 | 2.22 | 1.50 |

The controller maintained all three attitude axes within the predefined error limits. However, because this experiment was conducted under a different wind speed from the lower-wind LQR experiment, these data are presented only as an independent LQR-I performance evaluation rather than as a direct controller comparison.

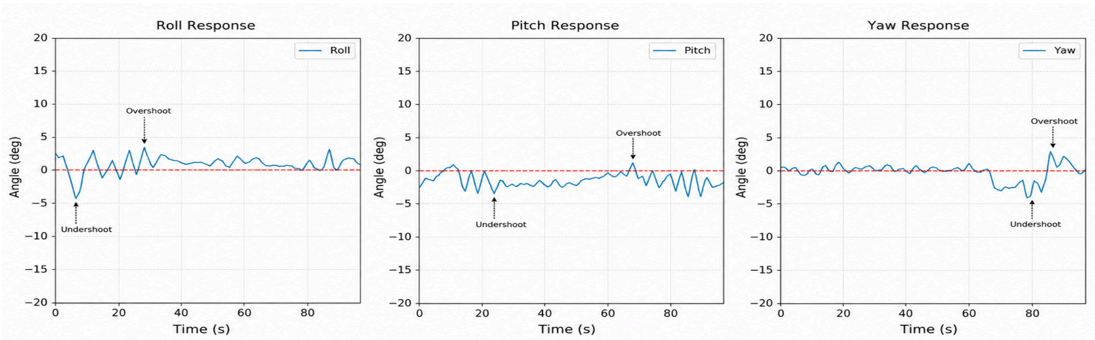


**Fig. 12** Roll, pitch, and yaw response using LQR-I under a wind speed of 2.6 m/s

### 3.4.2 Flight Test at 4.4 m/s Wind Speed

The LQR-I controller was subsequently evaluated under the same measured wind speed of 4.4 m/s used in the principal conventional-LQR experiment.

**Table 5**. LQR-I Flight Performance Under a Wind Speed of 4.4 m/s

| Parameter | Roll | Pitch | Yaw |
|---|---|---|---|
| Overshoot (°) | 5.47 | 2.85 | 3.35 |
| Steady-State Error (°) | 0.83 | -2.03 | 0.89 |
| RMSE (°) | 2.07 | 2.54 | 1.23 |

The highest overshoot occurred on the roll axis at 5.47°, whereas the pitch and yaw overshoots were substantially smaller at 2.85° and 3.35°, respectively. The RMSE values remained below those obtained using the conventional LQR for all three axes. In particular, the yaw RMSE decreased to 1.227°, indicating improved regulation of the servo-actuated yaw dynamics under the investigated disturbance condition.

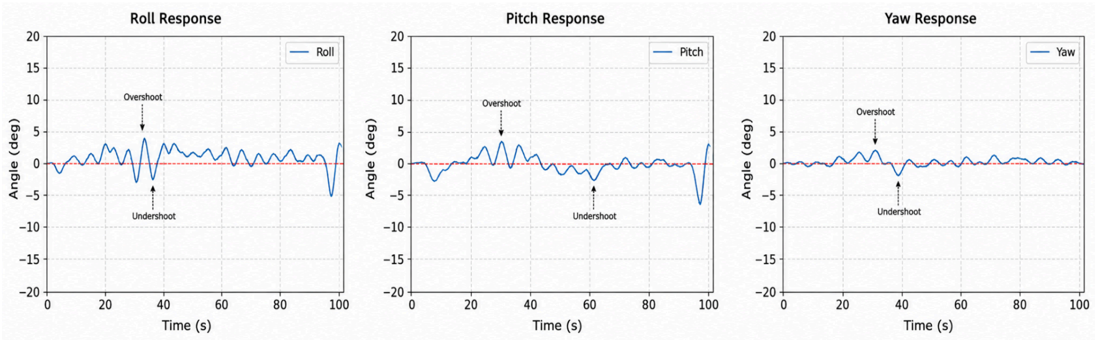


**Fig. 13** Roll, pitch, and yaw response using LQR-I under a wind speed of 4.4 m/s

### 3.4.3 Direct Comparison between LQR and LQR-I

A direct quantitative comparison was performed only using experiments conducted at the identical measured wind speed of 4.4 m/s. This approach reduces the influence of differences in disturbance magnitude on the comparison between controllers.

**Table 6**. Direct Comparison of LQR and LQR-I Under a 4.4 m/s Wind Disturbance

| Parameter | Controller | Roll | Pitch | Yaw |
|---|---|---|---|---|
| Overshoot (°) | LQR | 5.25 | 9.03 | 13.43 |
| | LQR-I | 5.47 | 2.85 | 3.35 |
| Steady-State Error (°) | LQR | 1.91 | 2.43 | 1.79 |
| | LQR-I | 0.83 | -2.03 | 0.89 |
| RMSE (°) | LQR | 2.45 | 3.39 | 2.74 |
| | LQR-I | 2.07 | 2.54 | 1.23 |

The strongest improvement was observed on the yaw axis. The yaw overshoot decreased from 13.43° to 3.35°, corresponding to a reduction of approximately 75.1%. Pitch overshoot decreased from 9.03° to 2.85°, corresponding to a reduction of approximately 68.4%.

In contrast, roll overshoot increased slightly from 5.25° to 5.47°, representing an increase of approximately 4.2%. This result demonstrates that integral augmentation did not uniformly reduce every transient-response metric. When the absolute magnitude of the steady-state error is considered, the roll error decreased from 1.909° to 0.8289°, corresponding to a reduction of approximately 56.6%. The pitch error magnitude decreased from 2.429° to 2.027°, corresponding to approximately 16.6%, while the yaw error decreased from 1.796° to 0.887°, corresponding to approximately 50.6%.

The RMSE decreased on all three rotational axes. Roll RMSE decreased from 2.451° to 2.065°, corresponding to an improvement of approximately 15.7%. Pitch RMSE decreased from 3.397° to 2.542°, corresponding to approximately 25.2%, while yaw RMSE decreased from 2.744° to 1.227°, corresponding to the largest reduction of approximately 55.3%.

The substantial improvement on the yaw axis is particularly relevant to the tricopter architecture. Unlike symmetric quadrotors, the tricopter generates yaw torque through the mechanical deflection of its rear propulsion unit. Servo nonlinearities, mechanical backlash, aerodynamic asymmetry, and persistent thrust-vector mismatch may therefore produce residual yaw deviations that are not fully compensated by conventional state feedback. The accumulated error term in LQR-I introduces an additional corrective action that can compensate for persistent bias.

The roll-axis response illustrates an important control trade-off. Although LQR-I reduced both the steady-state-error magnitude and RMSE, its peak roll overshoot increased slightly. Therefore, the effect of integral augmentation should not be interpreted as a uniform improvement in every transient parameter. Instead, the experimental results demonstrate an overall improvement in attitude-tracking accuracy and disturbance rejection, with particularly pronounced benefits in pitch and yaw regulation.

## 4. Conclusion

This study developed and experimentally evaluated an integral-augmented Linear Quadratic Regulator for attitude stabilization of a physical single-tilt tricopter UAV. The controller was implemented on an embedded flight controller and evaluated using repeated tuning-rig experiments followed by outdoor free-flight tests under measured natural wind disturbances. A conventional LQR controller was used as the baseline.

The tuning-rig experiments demonstrated that the LQR-I controller maintained relatively small steady-state attitude errors on all rotational axes. The yaw response was the most consistent, whereas the roll and pitch responses exhibited higher trial-to-trial variability in overshoot. These results demonstrate the importance of evaluating both steady-state and transient characteristics rather than relying on individual trials.

The principal direct comparison was conducted at an identical measured wind speed of 4.4 m/s. Under this condition, integral augmentation reduced pitch overshoot by approximately 68.4% and yaw overshoot by approximately 75.1%. Roll overshoot increased slightly by approximately 4.2%. Nevertheless, the magnitude of the steady-state error decreased by approximately 56.6%, 16.6%, and 50.6% for roll, pitch, and yaw, respectively.

The RMSE was reduced by approximately 15.7% for roll, 25.2% for pitch, and 55.3% for yaw. The largest overall improvement was therefore observed on the yaw axis, which is particularly significant for a tricopter because yaw regulation depends directly on the servo-actuated rear-rotor mechanism.

The results demonstrate that integral augmentation can improve the overall tracking accuracy and disturbance-rejection performance of LQR-based attitude control on a physical tricopter. However, the slight increase in roll overshoot and the variability observed during tuning also indicate that integral gain selection introduces a trade-off between steady-state accuracy and transient behavior.

Future work should investigate more systematic optimization of the LQR weighting matrices and integral gains, repeated flight experiments under controlled and repeatable wind disturbances, and longer-duration tests. Adaptive integral-gain adjustment or data-driven tuning methods may also be investigated to reduce transient variability while preserving the steady-state improvements achieved by integral augmentation.

## Author Contribution:

Dika Saputra: developed the hardware and software system, data collection, data analysis, interpretation of the results, and prepared the initial manuscript. Oktaf Agni Dhewa: preparation of the manuscript, and review and revision of the manuscript.

## Funding:

This research received no external funding.

## Acknowledgment:

The authors would like to thank all parties who provided support and assistance during the implementation of this research.

## Conflicts of Interest:

The authors declare no conflict of interest.

## References

[1] A. Khalid, Z. Mushtaq, S. Arif, K. Zeb, M. A. Khan, and S. Bakshi, “Control schemes for quadrotor UAV: Taxonomy and survey,” ACM Computing Surveys, vol. 56, pp. 1–32, 2023, doi: 10.1145/3617652.

[2] M. Ramp and E. Papadopoulos, “On modeling and control of a holonomic tricopter,” Journal of Intelligent & Robotic Systems, vol. 105, 2022, doi: 10.1007/s10846-021-01541-9.

[3] D. Abara, P. Bhowmick, and A. Lanzon, “A negative imaginary robust formation control scheme for networked multi-tilt tricopters utilizing an inner-loop sliding-mode control technique,” Automatica, vol. 169, Art. no. 111813, 2024, doi: 10.1016/j.automatica.2024.111813.

[4] M. Rinaldi, S. Primatesta, and G. Guglieri, “A comparative study for control of quadrotor UAVs,” Applied Sciences, vol. 13, no. 6, Art. no. 3464, 2023, doi: 10.3390/app13063464.

[5] M. Okasha, J. Kralev, and M. Islam, “Design and experimental comparison of PID, LQR and MPC stabilizing controllers for Parrot Mambo mini-drone,” Aerospace, vol. 9, no. 6, Art. no. 298, 2022, doi: 10.3390/aerospace9060298.

[6] G. Godínez-Garrido, O. Santos-Sánchez, H. Romero-Trejo, and O. García-Pérez, “Discrete integral optimal controller for quadrotor attitude stabilization: Experimental results,” Applied Sciences, vol. 13,

Art. no. 9293, 2023, doi: 10.3390/app13169293.

[7] S. M. Ahmad and S. Fareed, “Attitude modelling and real-time robust control of a 3-DoF quadcopter UAV test bench,” The Aeronautical Journal, 2024, doi: 10.1017/aer.2024.11.

[8] O. A. Dhewa and A. Nasuha, “Enhancement of stability on autonomous waypoint mission of quadrotor using LQR integrator control,” IIUM Engineering Journal, vol. 23, no. 1, pp. 129–158, 2022, doi: 10.31436/iiumej.v23i1.1803.

[9] O. A. Dhewa, F. Arifin, A. S. Priyambodo, A. Winursito, and Y. M. Mustafa, “Attitude UAV stability control using Linear Quadratic Regulator-Neural Network (LQR-NN),” IIUM Engineering Journal, vol. 25, no. 2, pp. 246–265, 2024, doi: 10.31436/iiumej.v25i2.3119.

[10] A. S. Elkhatem and S. N. Engin, “Robust LQR and LQR-PI control strategies based on adaptive weighting matrix selection for a UAV position and attitude tracking control,” Alexandria Engineering Journal, vol. 61, no. 8, pp. 6275–6292, 2022, doi: 10.1016/j.aej.2021.11.057.